JOURNAL OF APPLIED ELECTROCHEMISTRY 17 (1987) 261–269

*Formation of corrosion-resistant layers by electrodeposition of refractory metals or by alloy electrowinning in molten fluorides**

PIERRE TAXIL, JEAN MAHENC

Laboratoire de Chimie Physique et d'Electrochimie, Laboratoire Associé au CNRS UA 192, Université Paul Sabatier, 118 route de Narbonne, 31062 Toulouse Cedex, France

Received 10 April 1986

The electrolytic treatment of less resistant metals such as iron, copper and nickel with tantalum or niobium has been carried out in K_2TaF_7–LiF–NaF or K_2NbF_7–LiF–NaF solutions in the 550 to 1050° C temperature range. Two kinds of experiments have been used.

(i) At lower temperatures, electroplating with pure tantalum and niobium on inert cathodes was performed. The electrodeposition mechanism of each metal was studied and coherent electroplates were prepared which were tested in electrocatalytic applications.

(ii) At higher temperatures (850–1050° C), using nickel cathodes, intermetallic compounds were obtained at more positive potentials than that for pure electrodeposition (Ta_2Ni, TaNi, $TaNi_2$, $TaNi_3$, NbNi, $NbNi_3$). The electrowinning of stable $TaNi_3$ and $NbNi_3$ layers was carried out by the metalliding process which makes these materials resistant to corrosion in various media. Further, a study of the kinetics of growth of the diffusion layer allowed a diffusion parameter to be determined which was in agreement with other results obtained by conventional methods.

1. Introduction

Molten fluorides are known as suitable media for both the electrodeposition of various metals [1] and the electrowinning of alloys by the metalliding process [2]. In this work, refractory metals (tantalum and niobium) are either electrodeposited as pure layers on less resistant metals or metallided as alloy layers. The experimental conditions are somewhat different in each case.

Previous investigations concerning the mechanism of reduction of the discharging ions show some particularities due to alloy formation and help to define the appropriate conditions for each type of process. Here, the following characteristics are examined:

(i) In the case of pure tantalum or niobium deposits, the crystal growth at the surface of the cathode must be taken into account. If high electrodeposition rates are applied the reduction process is controlled by diffusion, so tertiary current distribution takes place and leads to dendritic formations. Nevertheless, pulsed electrolysis was shown to be able to overcome this difficulty. The main electrochemical applications of these coatings are related to the good stability of the oxides Ta_2O_5 or Nb_2O_5. After anodizing in dilute phosphoric solutions, a material for use in electrolytic capacitors is obtained. On the other hand, further platinizing treatment of the refractory metal coating leads to a new type of anode for gas production by electrolysis.

(ii) Surface alloys can be obtained if nickel is used as the cathode and the temperature is raised above 800° C. The layer consists only of stable $TaNi_3$ and $NbNi_3$ phases even if other metastable compounds can be observed at the surface of the cathode during the process.

The tantalum and niobium–nickel alloys prepared elsewhere by metallurgical techniques

* This paper was presented at a workshop on the electrodeposition of refractory metals, held at Imperial College, London, in July 1985.

0021–891X/87 $03.00 + .12 © 1987 Chapman and Hall Ltd.

have been shown to be sufficiently corrosion-resistant to be used as insoluble anodes [3–5]. It will be shown that the same applications can be expected for the surface alloys derived from the metalliding process.

2. Experimental details

2.1. *Technical*

The cell consisted of a refractory steel lid placed in a regulated furnace and provided with a vacuum supply and an argon gas circuit. The device has been described elsewhere [6, 7]. The melt was previously dehydrated by slow fusion under vacuum followed by bubbling with argon gas for 16 h. All the experiments were performed under an argon atmosphere.

A multipurpose electrochemical installation was used, based on a Tacussel PRT 20 10X potentiostat monitored by a periodic triangular signal generator (Tacussel model GSTP). Voltammograms, chronoamperograms and chronopotentiograms were recorded with an X–Y recorder, a Schlumberger storage oscilloscope or a Tacussel recorder type EPL1. The micrographic analysis was performed by means of an electronic microscope and an X-ray microprobe.

2.2. *Salts*

The electrolytic bath consisted of a solution of K_2TaF_7 or K_2NbF_7 in the eutectic melt LiF–NaF–KF (freezing point 460° C) or LiF–NaF (freezing point 650° C).

A single valence (5) is noted for tantalum ions in the fluoride melt. Two valences are considered in the case of niobium solutions, according to the following equilibrium:

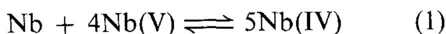

$$\mathrm{Nb} + 4\mathrm{Nb(V)} \rightleftharpoons 5\mathrm{Nb(IV)} \quad (1)$$

In order to obtain good cathodic efficiencies in the electrodeposition process a valence of niobium ions close to 4 is required; a further addition of metallic niobium in the bath displaces Equilibrium 1 to the right and leads to an average valence of 4.2 [8].

2.3. *Electrodes*

The working electrodes (cathodes) were wires (ϕ = 1 mm) or sheets (width 0.75 or 1.5 cm) of noble metals such as molybdenum, stainless steel, copper or nickel. The first three metals were used if no alloy formation was required, as the use of nickel leads to various intermetallic compounds with tantalum or niobium above 800° C [9].

The counter electrode (anodes) were graphite rods (ϕ = 4 mm) or, in the case of coating production, two foils of tantalum or niobium placed on each side of the cathode.

Various types of reference electrodes were used: a tantalum wire in solutions of tantalum ions (indicator of the Ta(V)–Ta reversible system) and a red-ox electrode M, Nb(V)–Nb(IV) (with M = molybdenum, copper or niobium) in solutions of niobium ions [10] are suitable. Furthermore, in some cases the more universal Ni(II)–Ni electrode, sheathed in boron nitride, was used. This electrode, prepared in our laboratory, was previously tested at 750° C in molten LiF–NaF [11].

3. Electrodeposition mechanism

3.1. *Investigations on inert cathodes*

The reduction of the refractory ions was studied by voltammetry, chronopotentiometry and chronoamperometry [12, 13]. Fig. 1 shows a voltammogram of molten LiF–NaF–K_2NbF_7 at 750° C for the case of a niobium ion valence close to 5. The following mechanism is proposed:

$$\mathrm{Nb(V)} + e \rightleftharpoons \mathrm{Nb(IV)} \quad (2)$$

$$\mathrm{Nb(IV)} + 4e \rightleftharpoons \mathrm{Nb} \quad (3)$$

at potentials of about −0.06 V and −0.17 V, respectively, referred to the Ni(II) (X = 0.01)–Ni system.

The formation of niobium crystals at potentials more negative than −0.156 V was confirmed by EDAX analysis and photomicrographs of the molybdenum cathode after potentiostatic electrolysis [12]. The reduction of tantalum ions is shown in Fig. 2 by voltammetry in quasi-

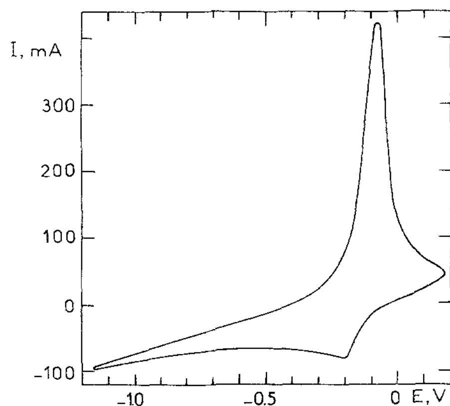

Fig. 1. Typical voltammogram of molten LiF–NaF–K_2NbF_7 at 750°C with a NiF_2 (X = 0.01)–Ni reference electrode. $C_{K_2NbF_7}$ = 5.85 × 10^{-5} mol cm^{-3}; cathodic area, A = 0.785 cm^2; potential sweep rate, v = 0.056 V s^{-1}.

stationary conditions at 560° C in molten LiF–NaF–KF, and on Fig. 3 by reversed chronopotentiometry. The reduction wave and the potential–time curve of the reducing step in the chronopotentiogram obey, respectively, the following equations:

$$E = \text{constant} + \frac{RT}{nF} \ln (i_L - i) \quad (4)$$

where n is the number of electrons, i_L the limiting current and i the current in the wave.

$$E = \text{constant} + \frac{RT}{nF} \ln (\tau^{1/2} - t^{1/2}) \quad (5)$$

where τ is the transition time and t the time before τ. The number of electrons involved is

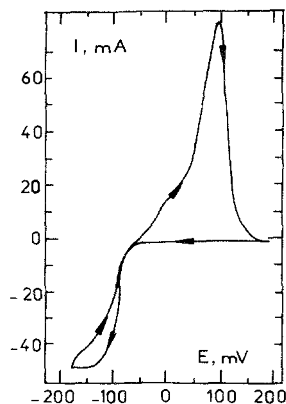

Fig. 2. Voltammogram of tantalum ions in molten LiF–NaF–KF at 550°C. Reference potential, tantalum wire; potential sweep rate, 1 mV s^{-1}.

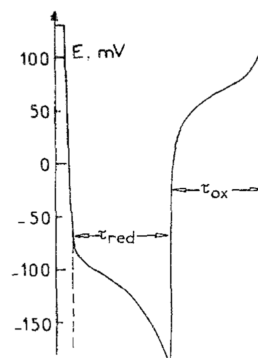

Fig. 3. Reversed chronopotentiogram of tantalum (V) ions in molten LiF–NaF at 800° C. $C_{K_2TaF_7}$ = 2.92 × 10^{-4} mol cm^{-3}; i = 100 mA cm^{-2}; reference potential, tantalum wire.

found to be close to five [13]. Thus reduction of tantalum ions involves only one step

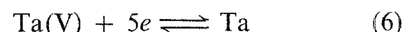

$$\text{Ta(V)} + 5e \rightleftharpoons \text{Ta} \quad (6)$$

at approximately −50 mV versus the tantalum reference electrode. Table 1 gives the values of the diffusion coefficients, $D_{Nb(VI)}$ and $D_{Ta(V)}$, obtained at different temperatures after the electrochemical measurements.

3.2. *Investigations on a nickel cathode at high temperatures*

When a nickel cathode is used and the temperature raised above 800° C, intermetallic diffusion of the cathodic and anodic metals takes place and can be demonstrated. Thus, the voltammogram of the molten LiF–NaF–KF–K_2TaF_7 at 1050° C on a nickel cathode shows some current peaks and plateaux which are characteristic of intermetallic compound formation between 0 and 250 mV versus the tantalum reference (Fig. 4). In the case of the molybdenum cathode, for which no intermetallic diffusion takes place, only the nucleation step is observed.

The potentials of formation of the nickel–tantalum compounds were accurately deter-

Table 1. Values of $D_{Nb(IV)}$ and $D_{Ta(V)}$ with varying temperature

	560° C	*660° C*	*750° C*	*800° C*
$D_{Ta(V)} \times 10^6$ ($cm^2 s^{-1}$)	0.17	0.67	–	2.8
$D_{Nb(IV)} \times 10^6$ ($cm^2 s^{-1}$)	–	–	4.0	–

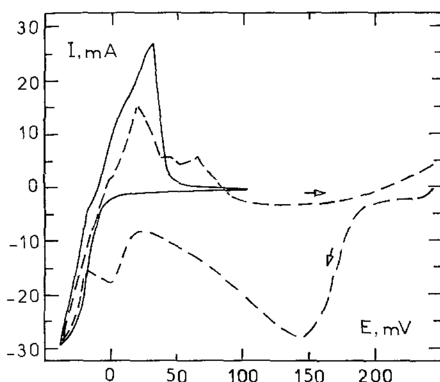

Fig. 4. Voltammogram of the LiF–NaF–K_2TaF_7 at 1050° C on different cathode materials. Reference potential, tantalum wire; potential sweep rate, 2 mV s^{-1}. Working electrodes: —— molybdenum; ----- nickel.

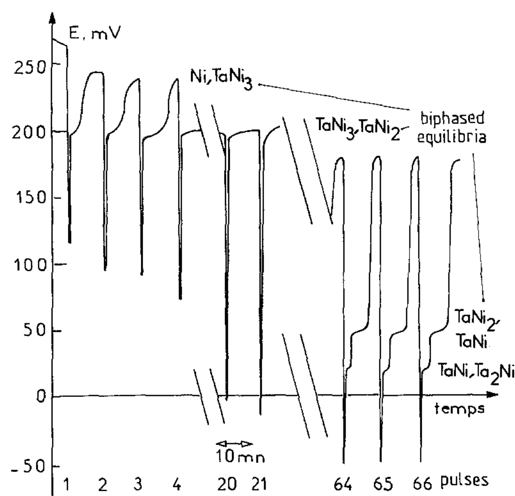

Fig. 5. Determination of the potentials of biphased equilibria of the tantalum–nickel system by a galvanostatic intermittent electrolysis. Duration of each pulse, 10 s; i = 16 mA cm^{-2}; t = 1050° C.

mined by potentiometric measurements after short cathodic galvanostatic pulses (Fig. 5). Between two pulses the diffusion of electrodeposited tantalum occurs and promotes a change in the composition of the external layer. Thus the evolution of the static potential exhibits several plateaux which are characteristics of biphased equilibria [10, 14].

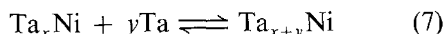

$$Ta_xNi + yTa \rightleftharpoons Ta_{x+y}Ni \qquad (7)$$

Therefore, the compounds of the tantalum–nickel system (Ta_2Ni, TaNi, $TaNi_2$ and $TaNi_3$) are formed at 20, 45, 200 and 245 mV versus the tantalum reference, respectively. These values are the e.m.f. of a cell

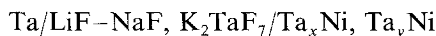

$$Ta/LiF\text{–}NaF,\ K_2TaF_7/Ta_xNi,\ Ta_yNi$$

which may be expressed as

$$\varepsilon = \mathring{\varepsilon} - \frac{RT}{5yF} \ln \frac{a_{Ta}(Ta_{x+y}Ni)}{a_{Ta}(Ta_xNi)} \qquad (8)$$

where a_{Ta} is the activity of tantalum in the solid phase and x and y are the stoichiometric coefficients involved in Equation 7.

It is thus possible to determine ΔG, the Gibbs energy of the tantalum–nickel alloys. Our values, presented in Table 2, agree with others obtained by e.m.f. measurements of solid galvanic cells carried out by Nesterenko *et al.* [15] and Lyakishev *et al.* [16].

The preceding results show that the intermetallic compounds can be obtained by electrolysis at a controlled potential, positive versus the tantalum or niobium reference, or by a galvanic technique: here, the metalliding reaction is achieved by an electrical connection between the refractory metal and the nickel cathode. In both cases the variation of the metalliding current with time shows an exponential decrease [7, 17]. This is due to diffusion control in the solid state.

Thus the mechanism involved, shown in Fig. 6, can be described by Fick's second law. It is assumed that the rate-determining step is the chemical diffusion within the layer and that the

Table 2. Values of energy of formation of tantalum–nickel intermetallic compounds

Compound	*Potential (mV) at 950° C*	*ΔG (kcal mol^{-1}) (present work)*	*ΔG (kcal mol^{-1}) (Ref. [15])*	*ΔG (kcal mol^{-1}) (Ref. [16])*
$TaNi_3$	≃245	−28.2	−26.89 (±6.76)	−31.7
$TaNi_2$	200	−25.7	−22.97 (±6.37)	−28.9
TaNi	45	−15.4	–	–
Ta_2Ni	20	−8.8	–	–

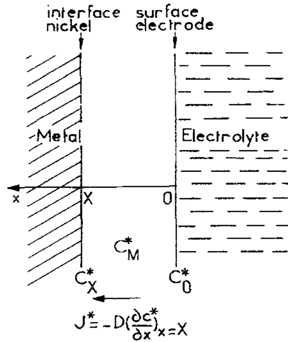

Fig. 6. Mechanism of the electrochemical formation of alloys by the metalliding process. J^*, Flux of diffusing species; C_0^*, C_X^*, C_M^*, composition of the alloy at $x = 0$, $x = X$ and the average composition, respectively.

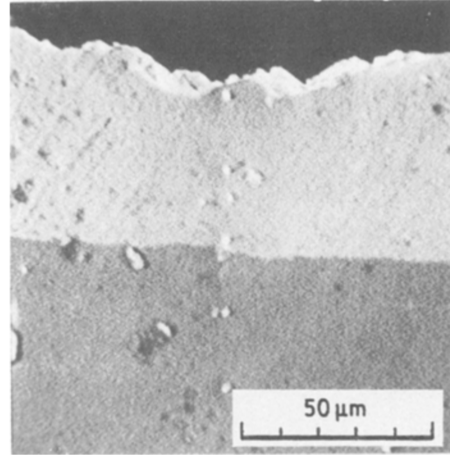

Fig. 7. SEM micrograph of the cross-section of a tantalum deposit on stainless steel.

mass transfer is controlled by the flux of the diffusing species at the nickel interface [7, 17, 18]. This leads to the following equation:

$$i = \frac{nFD^{*1/2}C_0^*}{\pi t^{1/2}} \exp\left\{-\left[\frac{X}{2(D^*t)^{1/2}}\right]^2\right\} \quad (9)$$

with $n = 4$ for niobium alloys and 5 for tantalum alloys, and where D^* is the intermetallic diffusion coefficient, C_0^* the refractory metal content at the surface of the cathode ($x = 0$) and X the thickness of the layer ($x = X$).

It is suggested elsewhere that X and D^* can be related by a parabolic relationship [19, 20],

$$X^2 = KT \quad (10)$$

where K is a constant, dependent on the temperature and proportional to D^*:

$$K = 4\alpha^2 D^* \quad (11)$$

where α is a constant [20].

Then, Equation 9 becomes

$$i = \frac{nFD^{*1/2}}{(\pi t)^{1/2}} C_0^* \exp(-\alpha^2) = p^* t^{-1/2} \quad (12)$$

According to potentiometric measurements [7, 17], the external composition of the alloy, C_0^*, is shown to correspond to Ta_2Ni (0.068 at g cm^{-3}) and NbNi (0.051 at g cm^{-3}). The average values of the slopes, p_{Ta}^* and p_{Nb}^*, at various temperatures are indicated in Table 3.

The step of alloy formation can be also identified by chronopotentiometric runs. When a low cathodic current is imposed at the nickel cathode, the potential stays at positive values for a time (τ^*) before decreasing more quickly towards negative values where nucleation occurs [7, 17]. It is assumed that τ^* is the time required to reach the saturation concentration, C_0^*, at the surface of the electrode. Thus, we have

$$i\tau^{*1/2} = \frac{nFC_0^* D^{*1/2}}{\pi^{1/2}} \exp(-\alpha^2) = p^* \quad (12')$$

The values of p^* obtained by this method are in agreement with those plotted in Table 3.

4. Electroplating with pure tantalum and nickel

4.1. *Characteristics of the process*

Several electroplates of pure tantalum and niobium on stainless steel, copper or nickel samples were prepared by means of galvanostatic elec-

Table 3. Values of p_{Nb}^* *and* p_{Ta}^* *with varying temperature*

	850° C	*900° C*	*940° C*	*950° C*	*1000° C*	*1050° C*
p_{Nb}^*(A cm^{-2} s$^{1/2}$)	0.061	0.068	0.098	–	0.115	0.164
p_{Ta}^*(A cm^{-2} s$^{1/2}$)	0.094	–	–	0.150	–	0.230

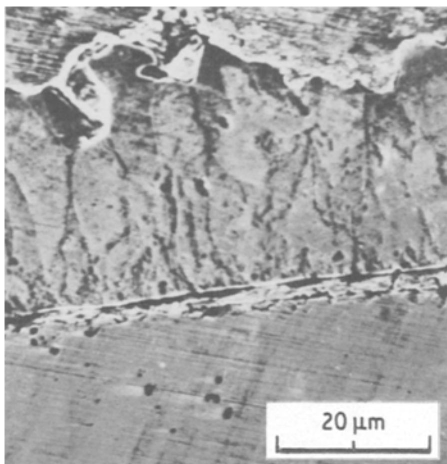

Fig. 8. SEM micrograph of a chemically attacked niobium deposit on nickel.

trolysis, then submitted to microscopic observation and analysis. Fig. 7 shows a SEM micrograph of the cross-section of a tantalum deposit on a stainless steel substrate. Good coherence and adherence of the layer is observed; the columnar structure is revealed after chemical attack by a $HF-H_2SO_4$ mixture (Fig. 8). The crystallized structure of the external surface is shown in Fig. 9.

The cathodic efficiency is always close to 100% in the case of tantalum electrodeposition. Moreover, high electrodeposition rates (100 μm per hour) can be obtained without the deleterious effect of dendritic formations.

Poorer cathodic efficiencies at low current densities are obtained for niobium electroplating even in reduced solutions of NbF_7^{2-}. This relates to the reversibility of the Nb(IV)–Nb system observed in Fig. 1. High current densities allow good efficiencies, but poor current distributions

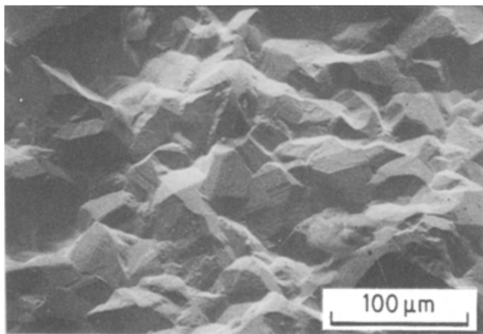

Fig. 9. SEM micrograph of the surface of a tantalum deposit.

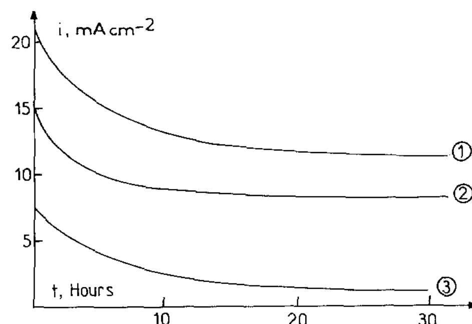

Fig. 10. Oxygen evolution in 0.5 M H_2SO_4 on platinized tantalum or niobium coatings at 1.95 V versus RHE 1, Sputtered platinum (0.5 μm); 2, sputtered platinum (0.2 μm); 3, electroplated platinum ($\simeq 7.5\ \mu$m).

occur due to a cathodic reaction controlled by diffusion, and this promotes dendritic growth. In order to avoid dendritic formations in high-rate electrodeposition of metals, several techniques involving the use of periodic currents have been proposed.

(i) In the periodic reverse electrolysis technique used by Cohen in niobium electrodeposition [21], the cathodic pulses were separated by anodic steps during which the deposit was polished.

(ii) The intermittent electrolysis technique, successfully performed by Ibl [22] in aqueous media, consisted of short cathodic pulses separated by relatively long off-times. The average current density over one period was close to the limiting current and the duration of the pulse was much less than the transition time.

4.2. *Applications*

Some properties of the refractory metal coatings were examined. They are not attacked by con-

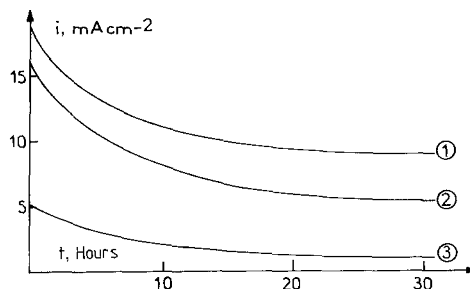

Fig. 11. Chlorine evolution in 1 M NaCl on platinized electrode, tantalum on niobium coatings at 1.55 V versus RHE. Conditions for curves 1 to 3 as for Fig. 10.

centrated alkali and acids except HF. Anodizing experiments in H_3PO_4 solutions provide dielectric layers of Ta_2O_5 (average value of $\varepsilon = 25.8$) on tantalum coatings. A further platinizing treatment of the coating by aqueous electrolysis or by sputtering leads to new types of insoluble anode which can be used in aqueous solutions of NaCl or H_2SO_4 at potentials of O_2 or Cl_2 evolution, and are capable of ensuring the production of these gases (Figs 10 and 11).

Figs 10 and 11 show the better catalytic effect of sputtered platinum compared with electrodeposited platinum. Other techniques such as painting with organometallic compounds have been shown to be more efficient [23, 24]. An important improvement in the properties of such anodes can be expected from the use of these techniques.

5. Tantalum–nickel and niobium–nickel surface alloy electrowinning

5.1. *Determination of kinetic parameters of the diffusion*

According to [3], surface alloys can be readily prepared under potentiostatic or galvanic conditions. Another technique consists of a mixed electrodeposition–diffusion process: the refractory metal is firstly electrodeposited in a galvanostatic electrolysis then diffuses in the nickel substrate. Complete diffusion is achieved when the potential of the electrode is 200 mV versus the tantalum reference or 30 mV versus the niobium reference. The weight of the diffused metal, Δm, was determined afterwards. The results are in agreement with the theoretical values calculated from Faraday's law. A linear relationship between $\Delta m/S$ (where S is the surface of the metallided sample) and the square root of time is demonstrated by Figs 12 and 13. The X-ray analysis of the layer with the microprobe shows that the composition of the layer is uniform and corresponds to $TaNi_3$ and $NbNi_3$ compounds.

The two preceding observations confirm the applicability of Equation 10 in our experimental results. The values of K are deduced from the slopes of the straight lines of Figs 12 and 13 from the densities of the $TaNi_3$ and $NbNi_3$ phases.

The values of K_{Ta} and K_{Nb} are given in Table 4. It is possible to calculate α after combining Equations 11 and 12:

$$\frac{\exp(-\alpha^2)}{\alpha} = \frac{2\pi^{1/2}p^*}{nFC_0^*K^{1/2}} \qquad (13)$$

The value of α is confirmed to be independent of temperature. The average values of α_{Ta} and α_{Nb} are 0.70 and 0.64 respectively. Thus, the intermetallic diffusion coefficient can be calculated from Equation 11. The values so obtained obey the Arrhenius law:

$$D_{Ta}^* = 1.1 \times 10^{-6} \exp\left(-\frac{10\,900}{T}\right) \text{cm}^2\text{s}^{-1} \qquad (14)$$

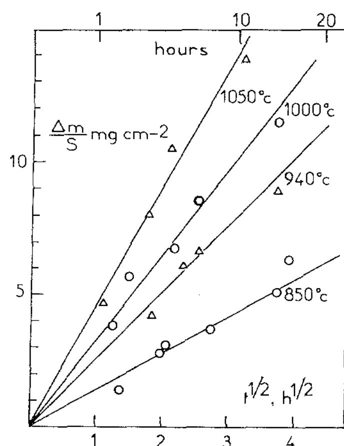

Fig. 12. Linear relationship betwen $\Delta m/S$ and the square root of time for metalliding with niobium at several temperatures.

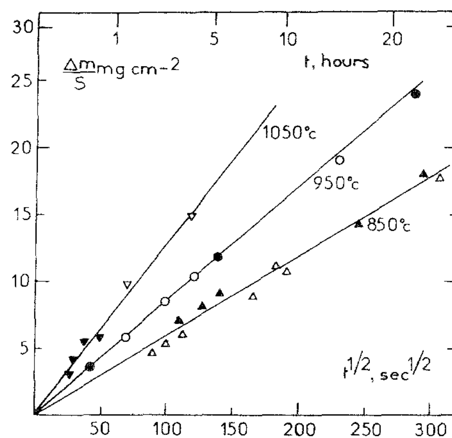

Fig. 13. Linear relationship between $\Delta m/S$ and the square root of time for metalliding with tantalum at several temperatures. ▼, ●, ▲: Galvanostatic technique; ▽, ○, △: potentiostatic technique.

Table 4. Values of K_{Nb} *and* K_{Ta} *with varying temperature*

	850° C	*940° C*	*950° C*	*1000° C*	*1050° C*
$K_{Nb} \times 10^{10}$ ($cm^2 s^{-1}$)	0.58	1.93	–	3.46	6.91
$K_{Ta} \times 10^{10}$ ($cm^2 s^{-1}$)	1.3	–	2.6	–	5.9

$$D^*_{Nb} = 1.3 \times 10^{-4} \exp\left(-\frac{16\,700}{T}\right) \text{cm}^2\,\text{s}^{-1} \quad (15)$$

The values of D^*_{Nb} are in agreement with other results provided from conventional techniques [25]. No reference was found in the literature for D^*_{Ta}.

5.2. *Corrosion resistance of the metallided samples*

The metalliding treatment by refractory metals causes nickel to have very high corrosion resistance in aqueous media at the potential of Cl_2 or O_2 evolution. This property is demonstrated by Figs 14 and 15 in which the anodic behaviour of some metallided samples in 0.5 M H_2SO_4 and 1 M NaCl, respectively, is compared with that of nickel and platinum. The passivation of the metallided samples is thought to derive from a stable mixed oxide NiO, Ta_2O_5 or NiO, Nb_2O_5 [26], which prevents the anodic dissolution of the metal and promotes gas evolution. This behaviour, similar to that of platinum, makes it possible to envisage the use of the surface alloys tantalum–nickel and niobium–nickel as anodes in gas production.

6. Conclusion

The treatment of common metals by refractory metals in molten fluorides presents two practical advantages.

1. In the case of inert cathodes such as stainless steel and copper it leads to an adherent, coherent and crystallized coating, able to be used in the same kind of applications as the solid

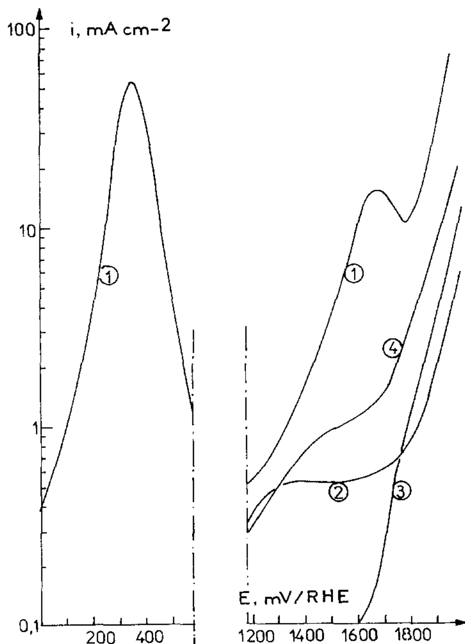

Fig. 14. Anodic polarization curves of nickel, platinum and metallided nickel samples in 0.5 M H_2SO_4 1, nickel; 2, niobided nickel; 3, tantalided nickel; 4, platinum.

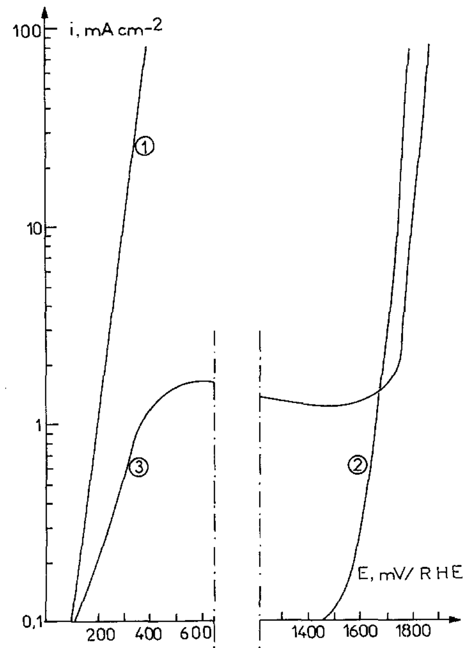

Fig. 15. Anodic polarization of nickel, platinum and metallided nickel samples in 1 M NaCl (1, nickel; 2, platinum; 3, niobided nickel).

refractory metals, such as electrolytic capacitors and catalysis.

2. When nickel is used as substrate, the coating can be completely diffused and then consists of surface alloys. Considering the high melting point of these alloys, their preparation by electrolysis at about 1000° C is particularly attractive and leads to new materials which can be used as insoluble anodes.

References

[1] R. S. Sethi, *J. Appl. Electrochem.* **9** (1979) 411.
[2] N. C. Cook, *Sci. American* **221** (1969) 38.
[3] G. N. Trusov, E. P. Gochalieva, B. A. Goncharenko and V. S. Mikhaeev, *Electrokhimiya* **13** (1977) 7, 1056.
[4] T. Fujii and H. Baba, *Boshoku Gijutsu* **29** (1980) 9, 457.
[5] *Idem, Jpn Kokai Tokyo Koh* 7947 812, 14 April 1979.
[6] P. Taxil and J. Mahenc, *Corr. Sci.* **21** (1981) 31.
[7] P. Taxil, *J. Less Common Metals* **113** (1985) 89.
[8] G. W. Mellors and S. Senderoff, *J. Electrochem. Soc.* **112** (1965) 266.
[9] M. Hansen and K. Anderko, 'Constitution of Binary Alloys', McGraw Hill, New York (1958).
[10] U. Cohen, PhD Dissertation, Standord, USA (1977).
[11] P. Taxil and Z. Y. Qiao, *J. Chim. Phys.* **82** (1985) 83.
[12] Z. Y. Qiao and P. Taxil, *J. Appl. Electrochem.* **15** (1985) 259.
[13] P. Taxil, Thesis, Toulouse (1986).
[14] A. Brenner, 'Electrodeposition of Alloys', Vol. 1, Academic Press, New York (1963).
[15] S. N. Nesterenko, L. L. Meshkov and C. M. Sokolovskaya, *Vest. Mosk. Univ. Ser. 2 Khim.* **22** (1981) 305.
[16] N. P. Lyakishev, Yu. P. Snitko and V. I. Alekseiev, *Dokl. Akad. Nauk. SSSR* **258** (1981) 1404.
[17] P. Taxil and Z. Y. Qiao, *J. Appl. Electrochem.* **15** (1985) 947.
[18] J. Crank, 'The Mathematics of the Diffusion', Oxford University Press, London (1964).
[19] W. Jost, 'Diffusion in Solids, Liquids, Gases', Academic Press, New York (1960).
[20] P. V. Danckwerts, *Trans. Faraday Soc.* **46** (1950) 701.
[21] U. Cohen, *J. Electrochem. Soc.* **128** (1981) 731.
[22] N. Ibl, J. C. Puippe and H. Angerer, *Surf. Technol.* **6** (1978) 287.
[23] G. Lodi, F. Silvieri, A. De Battesti and S. Trasatti, *J. Appl. Electrochem.* **8** (1978) 135.
[24] R. Kotz, H. J. Lewerenz and S. Stucki, *J. Electrochem. Soc.* **130** (1983) 825.
[25] Y. Muramatsu, *Trans. Nat. Res. Inst. Met.* **17** (1975) 21.
[26] M. P. Arbusov and V. G. Chuprina, *Poroshk Metall. (Kiev)* (1978) **2**, 72.